Biochemical and Biophysical Research Communications 384 (2009) 120–125

Contents lists available at ScienceDirect

Biochemical and Biophysical Research Communications

journal homepage: www.elsevier.com/locate/ybbrc

# OCT4A contributes to the stemness and multi-potency of human umbilical cord blood-derived multipotent stem cells (hUCB–MSCs)

Kwang-Won Seo [a,b,1], Sae-Rom Lee [a,b,1], Dilli Ram Bhandari [a,b], Kyoung-Hwan Roh [a,b], Sang-Bum Park [a,b], Ah-Young So [a,b], Ji-Won Jung [a,b], Min-Soo Seo [a,b], Soo-Kyung Kang [a,c], Yong-Soon Lee [a,b], Kyung-Sun Kang [a,b,*]

[a] Adult Stem Cell Research Center, College of Veterinary Medicine, Seoul National University 151-742, Seoul, Republic of Korea
[b] Laboratory of Stem Cell and Tumor Biology, Department of Veterinary Public Health, College of Veterinary Medicine, and BK21 Program for Veterinary Science, Seoul National University 151-742, Seoul, Republic of Korea
[c] Laboratory of Biotechnology, College of Veterinary Medicine, and BK21 Program for Veterinary Science, Seoul National University 151-742, Seoul, Republic of Korea

ARTICLE INFO

*Article history:*
Received 13 April 2009
Available online 24 April 2009

*Keywords:*
OCT4
Umbilical cord blood-derived mesenchymal stem cells
shRNA
Stemness
Multi-potency

ABSTRACT

The *OCT4A* gene, a POU homeodomain transcription factor, has been shown to be expressed in embryonic stem cells (ESC) as well as hUCB–MSCs. In this study, the roles played by OCT4A in hUCB–MSCs were determined by stably inhibiting OCT4A with lenti-viral vector-based small hairpin RNA (shRNA). A decreased rate of cell proliferation was observed in OCT4-inhibited hUCB–MSCs. Down-regulation of *CCNA2* expression in OCT4-inhibited hUCB–MSCs was confirmed by RT-PCR and real-time RT-PCR analysis in three genetically independent hUCB–MSC clones. Adipogenic differentiation was also suppressed in OCT4-inhibited hUCB–MSCs. The up-regulation of *DTX1* and down-regulation of *HDAC1, 2,* and *4* expressions may be related to this differentiation deformity. The expression of other transcription factors, including *SOX2*, *REX1* and *c-MYC*, was also affected by OCT4 inhibition in hUCB–MSCs. In conclusion, these finding suggest that OCT4A performs functionally conserved roles in hUCB–MSCs, making its expression biologically important for *ex vivo* culture of hUCB–MSCs.



## Introduction

Multipotent stem cells or mesenchymal stem cells (MSCs) can be isolated from various tissues, including bone marrow, adipose tissue, peripheral blood, fetal liver, lung, amniotic fluid, chorion of placenta and umbilical cord blood (UCB) [1–4]. MSCs can be induced to differentiate into fibroblasts, adipocytes, osteoblasts, chondrocytes [5], tendinocytes, ligamentocytes [6], cardiomyocytes [7], neuronal cells [8,9] and other cell types [10]. MSCs are currently thought to be excellent candidate tools for the field of regenerative medicine, as they have trophic effects, immunosuppressive effects and the ability to generate multiple cell lineages.

The functions of OCT4 in embryonic stem cells (ESCs) have been relatively well described in previous studies and Oct4 has been shown to be essential for the self-renewal and differentiation abilities of mammalian ESCs [11]. However, the precise expression patterns and functions of Oct4 in adult mammalian stem cells are still controversial [12]. Unlike ESCs, peripheral blood mononuclear cells produce an alternative *OCT4* transcript, referred to as *OCT4B* to distinguish it from the original form, *OCT4A*, and *OCT4B* does not share the stemness factor with *OCT4A* [13]. Lengner et al. have suggested that *Oct4*, a mouse homolog of human *OCT4A*, has no physiological function *in vivo* [12,14]. We hypothesized and tested whether OCT4A present in cultured human umbilical cord blood-derived multipotent stem cells (hUCB–MSCs) and have a function to multipotency of hUCB–MSCs, one of the youngest adult stem cell types.

## Materials and methods

*Isolation and culture of hUCB–MSCs.* The UCB samples were obtained from the umbilical vein immediately after delivery, with the informed consent of the mother approved by the Boramae Hospital Institutional Review Board (IRB) and the Seoul National University IRB. The UCB samples were mixed with Hetasep solution (StemCell Technologies, Vancouver, Canada) at a ratio of 5:1, and then incubated at room temperature to deplete erythrocyte counts. The supernatant was carefully collected and mononuclear cells were obtained using Ficoll density-gradient centrifugation at 2500 rpm for 20 min. The cells were washed once or twice in PBS and seeded at a density of $2 \times 10^5$ to $2 \times 10^6$ cells/cm$^2$ on plates in a humidified atmosphere of 5% $CO_2$ at 37 °C. Growth media consisted of D-media (Formula No. 78-5470EF, Gibco BRL, Grand Island, NY, USA) contain-

* Corresponding author. Address: Laboratory of Stem Cell and Tumor Biology, Department of Veterinary Public Health, College of Veterinary Medicine, and BK21 Program for Veterinary Science, Seoul National University, 151-742 Seoul, Republic of Korea. Fax: +82 02 876 7610.
*E-mail address:* kangpub@snu.ac.kr (K.-S. Kang).
[1] These authors contributed equally to this work.

0006-291X/$ - see front matter © 2009 Elsevier Inc. All rights reserved.
doi:10.1016/j.bbrc.2009.04.094

ing EGM-2 SingleQuot and 10% fetal bovine serum (Gibco BRL). After three days, non-adherent cells were removed. The adherent cells formed colonies and grew rapidly, exhibiting spindle-shaped morphology. The tera-1 cell line was purchased from ATCC (HTB-105, Manassas, VA, USA) and maintained in DMEM low glucose medium (Gibco BRL) plus 10% FBS (Gibco BRL). The human fibroblast was purchased from KCLB (CCD-986SK, Seoul, Korea).

*Fluorescence-activated cell sorting (FACS) analysis.* To analyze cell surface marker expression in hUCB–MSCs, FACSAria was used (Becton & Dickinson, Franklin Lakes, NJ, USA). Briefly, hUCB–MSCs were fixed with 70% ethanol for 10 min at 4 °C and stained for 30 min on ice with anti-human antibodies that recognize various surface molecules: Antibodies were conjugated to CD14-fluorescein isothiocyanate (FITC) (Abcam, Cambridge, UK), CD24-phycoerythrin (PE), CD29-PE, CD31-PE, CD34-FITC, CD44-PE, CD45-FITC, CD62P-PE, CD73-PE, CD90-PE, CD105-FITC, CD133-PE, HLA-DR-FITC, and human Octamer-4 (*OCT-4*)-PE (Becton & Dickinson).

*Production of lentiviral vectors.* Lenti-viruses were generated using ViraPower™ Lentiviral packaging mix (Invitrogen, Carlsbad, CA, USA). Lipofectamine 2000 (Invitrogen) was used for transfection of SHDNAC-TRCN0000004881 (OCT4sh1), SHDNAC-TRCN0000 004882 (OCT4sh2), and SHC002 (random sequences inserted for vehicle control) (Sigma, Saint Louis, MO, USA) into 293FT cells (Invitrogen). The supernatant was harvested at 48 and 72 h after transfection. hUCB–MSCs were infected with 10 multiplicity of infection (MOI) of lenti-viruses. Polybrene (Sigma) was added to the culture media at a final concentration of 6 μg/ml. For selection, puromycin was added to the culture media at a final concentration of 3 μg/ml for three days.

*Induction of differentiation.* For adipogenic differentiation, cells were seeded and maintained at 80–90% confluency and incubated with DMEM low glucose medium (Gibco BRL), 10% FBS (Gibco BRL), 1 μM dexamethasone (Sigma), 10 μg/ml insulin (Sigma), 0.5 mM 3-isobutyl-1-methylxanthine (Sigma), and 0.2 mM indomethacin (Sigma) as reported by Okamoto et al. [15]. To induce osteogenic differentiation, cells were seeded and maintained at 70–80% confluency, and incubated with DMEM low glucose medium (Gibco-Invitrogen), 10% FBS (Gibco-Invitrogen), 0.1 μM dexamethasone (Sigma), 10 mM beta-glycerophosphate (Sigma), and 50 μM ascorbate (Sigma) [16]. For chondrogenic differentiation, cells were incubated with complete chondrogenic media (Cambrex Bio Science Inc, Walkersville, MD, USA).

*Cell cycle analysis.* Three days after infection, hUCB–MSCs were washed twice with PBS and harvested by trypsinization. The cells were then washed again with PBS and fixed with 70% ethanol at −20 °C for one day. The fixed cells were washed with ice-cold PBS and stained with 50 μg/ml propidium iodide (Sigma) in the presence of 100 μg/ml RNase A (Sigma) for 30 min. The cell cycle was analyzed using the FACSCalibur (Becton & Dickinson).

*RT-PCR and PCR array.* Total RNA was extracted with an easy-spin™ Total RNA Extraction Kit (Intronbio, Sungnam, Republic of Korea) according to the manufacturer's instructions. cDNA synthesis was carried out using the SuperScript® III First-Strand Synthesis Kit (Invitrogen) for RT-PCR with 1 μg total RNA. Primer sequences for each gene are shown in Supplementary Table 2. Gene expression was also analyzed using real-time PCR with SYBR Green Master Mix reagents (Applied Biosystems, Foster City, CA, USA). For the PCR array, 0.5 μg total RNA was reverse transcribed with a $RT^2$ First Strand Kit (SuperArray, Frederick, MD, USA). $RT^2$ Profiler Stem Cell PCR Array (Catalog No. PAHS-405, SuperArray) was performed according to the manufacturer's protocol. Real-time RT-PCR was performed with a LightCycler 489 Real-Time PCR System (Roche, Indianapolis, IN, USA). Three genetically independent hUCB–MSCs were analyzed for this experiment.

*Immunofluorescence staining of OCT4.* Cells were fixed with 4% paraformaldehyde for 20 min at room temperature and incubated with blocking solution (10% normal goat serum, Rockland Immunochemicals, Gilbertsville, PA, USA) overnight at 4 °C. Cells were then incubated overnight at 4 °C with primary antibodies against OCT4 (Catalog No. 19857, Abcam) diluted in blocking solution and then reacted with the Alexa Fluor 594 anti-rabbit IgG secondary antibody (Invitrogen) for 1 h. For nuclear counter-staining, Hoechst 33238 (1 μg/ml, Sigma) was applied at a dilution of 1:100 in PBS for 15 min. Images were taken with a confocal microscope (Eclipse TE200, Nikon, Tokyo, Japan). For Western blot analysis, the same primary antibody was used as FACS analysis (Abcam).

*Statistical analysis.* The change in the Ct (ΔCt) of the target genes was calculated as ΔCt = (Ct of target genes) – (Ct of GAPDH). The ratio of the target gene to the housekeeping gene was calculated and expressed as $2^{-\Delta Ct}$. This ratio was then used to evaluate the expression level within each target gene in *OCT4*-inhibited hUCB–MSCs and vehicle control-infected hUCB–MSCs. To determine the fold changes in gene expression, the normalized gene expression of the target genes in OCT4-inhibited hUCB–MSCs was divided by the normalized expression of the same target gene in the vehicle control samples, expressed as $2^{-\Delta\Delta Ct}$. The data from the quantitative RT-PCR were presented as mean value ± standard deviation from three genetically independent clones of hUCB–MSCs and Student's *t*-test was used for analysis and calculation of *p*-values.

## Results

### *OCT4A is expressed in hUCB–MSCs*

Isolated hUCB–MSCs expressed characteristic MSC antigens, including $CD29^+$, $CD44^+$, $CD73^+$, $CD90^+$, $CD105^+$, $CD34^-$ and $CD45^-$. In the differentiation studies of hUCB–MSCs, at least three cell lineages were observed following different induction protocols, including adipocytes, osteocytes and chondrocytes (data not shown). By immunofluorescence staining, OCT4 expression was found specifically in the nuclei of hUCB–MSCs (Fig. 1A). Seventy-three percentage of hUCB–MSCs under our culture conditions expressed OCT4 at passage 5 (Fig. 1B). The *OCT4A* specific amplicon was detected by RT-PCR analysis (Fig. 1C) when *OCT4A*-specific primer pairs were used [17]. However, *OCT4B* was not detected in hUCB–MSCs. Finally, a specific band corresponding to the molecular weight of OCT4A was revealed in hUCB–MSC but not in human fibroblast by Western blot analysis (Supplementary Figure 2C).

### *Inhibition of OCT4 expression resulted in growth retardation of hUCB–MSCs*

Three genetically independent clones of hUCB–MSCs were analyzed in each of the following experiments. The *OCT4* expression level was significantly reduced after infection with two different OCT4-inhibition-viruses as compared with the vehicle control-infected hUCB–MSCs, by both real-time and RT-PCR analyses (Fig. 2A). *OCT4* expression in OCT4sh2-infected hUCB–MSCs was reduced to approximately 35% of vehicle control-infected hUCB–MSCs. The cell proliferation rate of OCT4-inhibited hUCB–MSCs was also decreased as compared to that of vehicle control-infected hUCB–MSCs (Fig. 2B). FACS cell cycle analysis showed that in vehicle control-infected hUCB–MSCs, 63–66% of cells were in G0/G1 phase, 10% were in G2/M phase, and approximately 25% were in S phase (Fig. 2D). However, the percentage of S phase cells in the OCT4sh2 treated hUCB–MSCs was much lower (∼10%). Additionally, in OCT4sh2 treated hUCB–MSCs, 85% of cells were in G0/G1 phase while the percentage of cells in G2/M phase was similar to the vehicle control-infected hUCB–MSCs (Fig. 2C and D). These results were similar in OCT4sh1 treated hUCB–MSCs (Supplementary Figure 2A and B).

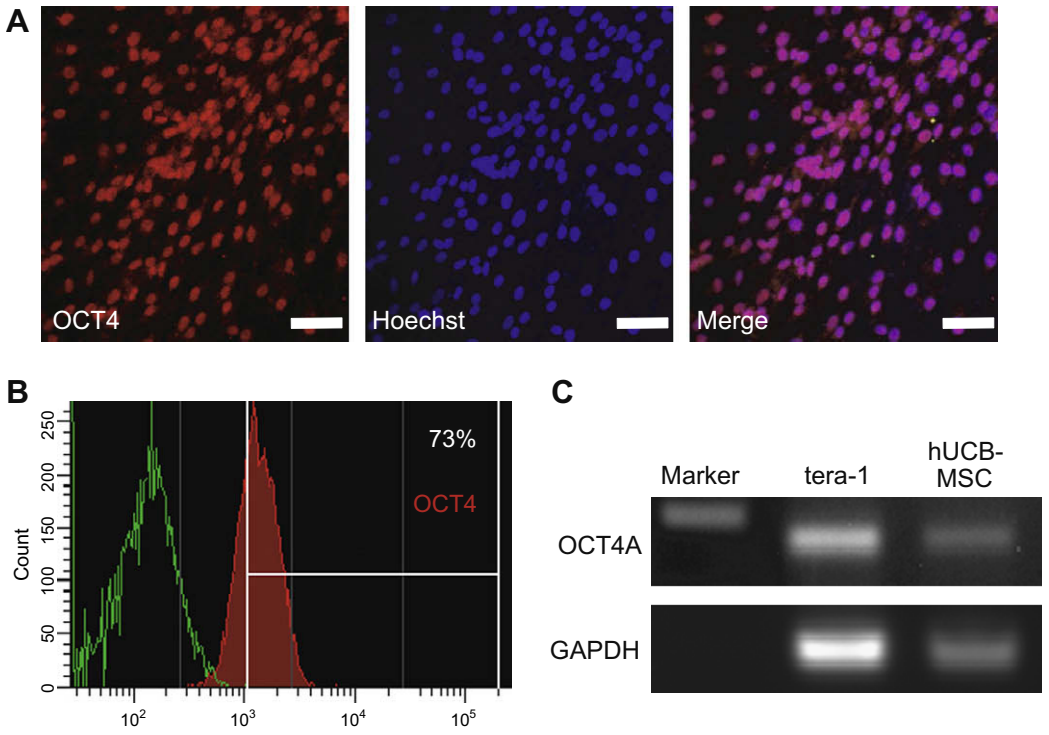


**Fig. 1.** OCT4A expression in hUCB–MSCs. (A) OCT4 was localized to the nuclei of hUCB–MSCs by immunofluorescence staining. (B) 73% of hUCB–MSCs were OCT4-positive according to FACS analysis. (C) The expression of *OCT4A* in hUCB–MSCs and the tera-1 cell line by RT-PCR analysis. Scale bar represents 100 μm.

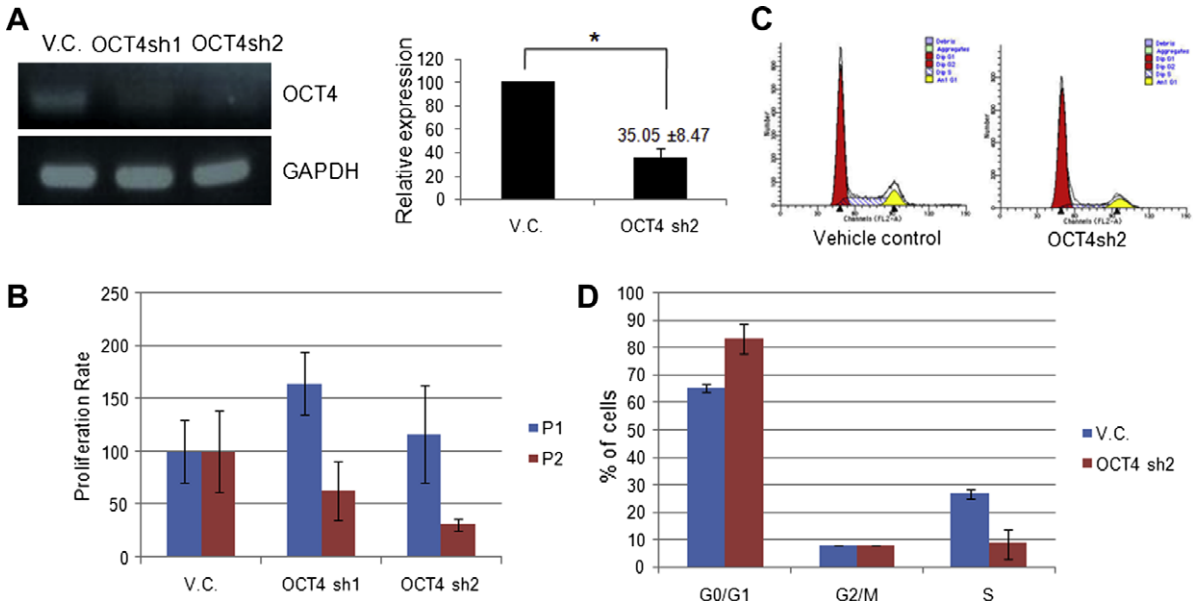


**Fig. 2.** Changes in cell proliferation rates after *OCT4* inhibition in hUCB–MSCs. (A) Real-time and RT-PCR analyses after shRNA lenti-viral infection (OCT4sh1, OCT4sh2) and vehicle control infection (VC). (B) Relative cell proliferation rates after lenti-viral infection. Plates were seeded with the same number of cells and counted at the end of each passage (P1, P2) after lenti-viral infection. (C and D) The effect of OCT4 inhibition on cell cycle progression of hUCB–MSCs. (C) Representative FACS data for vehicle control- and OCT4sh2-infected hUCB–MSCs. (D) The percentage of cells at each cell cycle stage as determined by FACS analysis after lenti-viral infection. $^{*}p < 0.05$.

*PCR array supported the growth retardation and cell cycle arrest of OCT4 inhibited hUCB–MSCs*

As two OCT4 knock-down virus showed similar phenotypes, one of two construct, which was OCT4sh2, was used in molecular study. The expression levels of 84 genes frequently cited in stem cell biology were examined by real-time RT-PCR (Supplementary Figure 1A). Three genes were up-regulated and nine genes were down-regulated in OCT4-inhibited hUCB–MSCs (Supplementary Table 1). For example, *CCNA2* and *MYST1* expression levels were 5-fold ($p = 0.006$) and 0.37-fold ($p = 0.019$) lower, respectively, in OCT4-inhibited hUCB–MSCs compared with the controls. *DTX1* and *FRAT1* expression levels were increased by 27.19-fold ($p = 0.015$) and 2.95-fold ($p = 0.043$), respectively, in OCT4-inhibited hUCB–MSCs relative to the vehicle control infected hUCB–MSCs (Supplementary Figure 1B–E).

*Inhibition of OCT4 expression disturbs the adipogenic differentiation of hUCB–MSCs*

No differences were found between the vehicle control-infected and OCT4-inhibited hUCB–MSCs after osteogenic induction (data not shown). However, adipogenic differentiation in OCT4-inhibited hUCB–MSCs was consistently delayed or repressed in every clone of hUCB–MSCs tested (Fig. 3). On the molecular level, the expression levels of two well known adipogenic marker genes, peroxisome proliferator-activated receptor gamma (*PPAR-γ*) and adipocyte fatty acid binding protein 2 (*AP2*), were tested. The significantly reduced expression of *PPAR-γ* in OCT4-inhibited hUCB–MSCs compared with the controls was found in two OCT4 knock-down constructs (Fig. 3B). Finally, the elution of Oil red O after staining showed that the optical density (OD) of the OCT4sh2-infected hUCB–MSCs was significantly lower than that of vehicle control infected hUCB–MSCs.

*Gene expression patterns were altered in OCT4-inhibited hUCB–MSCs*

The expression levels of transcription factors, *SOX2*, *REX1* and *c-MYC* as well as Polycomb group genes *SUZ12* and *BMI1*, were clearly reduced in OCT4-inhibited hUCB–MSCs as compared to the controls, according to RT-PCR analysis. However, the expression of *ZNF281* was not visibly changed. The expression of *CCNA2* was also reduced in OCT4-inhibited cells, which conformed to the results of the PCR array. Transcriptional changes in the histone deacetylase gene family (*HDAC*) were observed with real-time RT-PCR. *HDAC2* and *HDAC4* were significantly reduced in the OCT4-inhibited hUCB–MSCs relative to the vehicle control-infected hUCB–MSCs.

## Discussion

In this study, mononuclear cells were isolated from the cord blood of infants. These mononuclear cells formed colonies within the first few days of culture and grew more rapidly at later generations, adopting spindle-shaped morphologies under the proper culture conditions. The cells possessed the trans-differentiation capacity to form at least three lineages, including adipocytes, chondrocytes and osteocytes. A survey of cell surface antigens in these cells revealed the presence of several antigens characteristic of mesenchymal stem cells. Therefore, these mononuclear cells were named hUCB–MSCs. Many genes were expressed in hUCB–MSCs, including transcription factors. Among them, the expression of OCT4A was confirmed by RT-PCR, Western blot, immunohistological staining and FACS analysis (Fig. 1, Supplementary Fig. 2C).

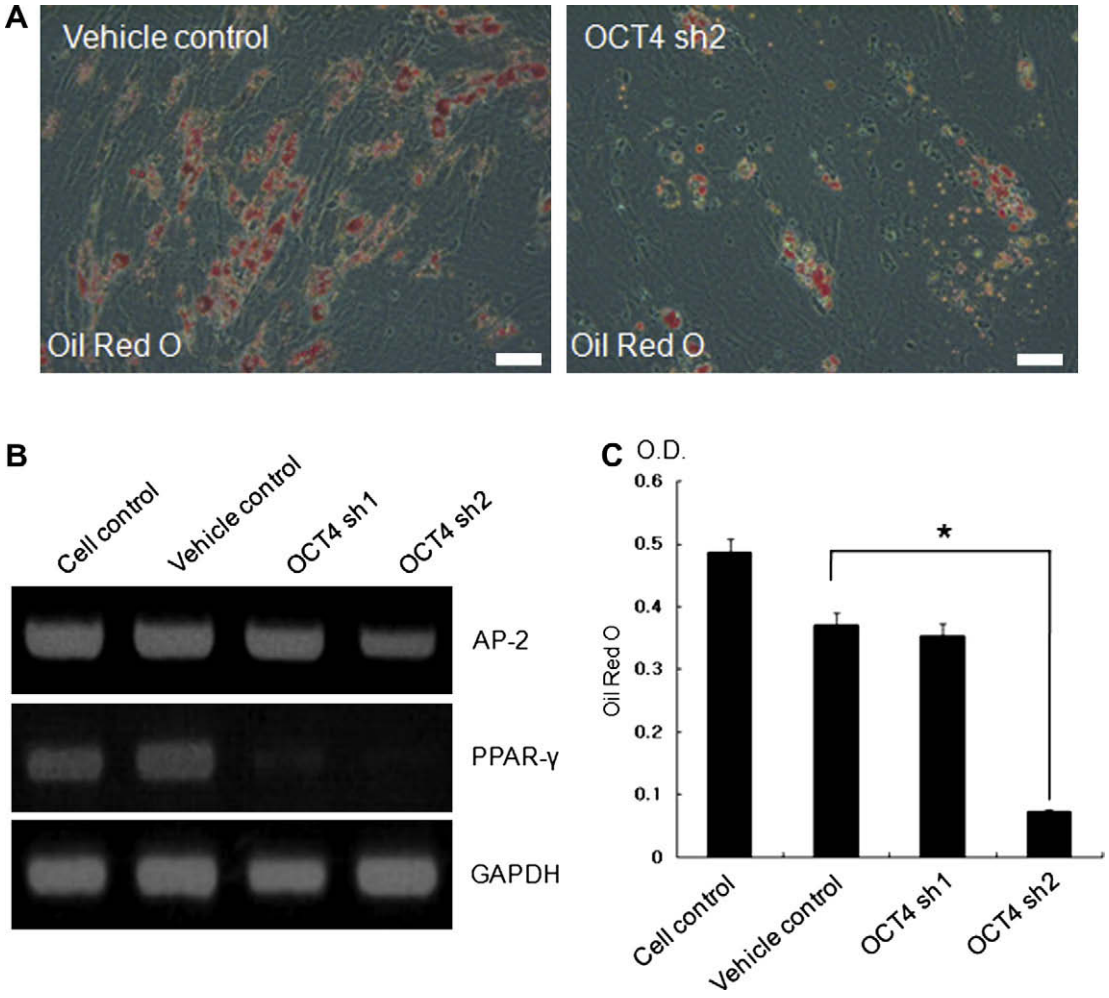


**Fig. 3.** Adipogenic differentiation after adipogenic induction. (A and C) Fifteen days after adipogenic induction, lipid droplet formation was determined by Oil Red O staining (A) and dye quantification after elution (C). Oil Red O stained cells and OD were significantly decreased in OCT4sh2-infected hUCB–MSCs compared to the vehicle control-infected hUCB–MSCs. (B) The expression levels of *AP2* and *PPAR-γ* were reduced in OCT4 inhibited hUCB–MSCs. GAPDH (glyceraldehydes-3′-phosphate dehydrogenase). *$p < 0.05$. Scale bar represents 100 μm.

OCT4A is a central regulator of ESC pluripotency. The exact expression pattern and function of OCT4A in somatic stem cells remain controversial [12]. There are many *OCT4* pseudogenes in the human genome. Therefore, specific RT-PCR primers were used in this experiment to avoid pseudogene detection or other false positive results [17]. OCT4A expression in hUCB–MSCs was confirmed by RT-PCR, Western blot and immunostaining despite the fact that this *OCT4A* expression level was not higher than in the tera-1 cell line.

The results from the cell proliferation assay indicate that OCT4 inhibition in hUCB–MSCs resulted in growth retardation. These results were further confirmed by cell cycle analysis. The proportion of S phase cells was decreased in the OCT4-inhibited hUCB–MSCs compared with the vehicle control-infected hUCB–MSCs. As a consequence, the percentage of G0/G1 phase cells was increased in the OCT4-inhibited cell lines (Fig. 2).

A PCR array for 84 genes referenced in stem cell biology was performed using real-time RT-PCR. Notably, *CCNA2* expression was significantly lower in the OCT4-inhibited hUCB–MSCs relative to the vehicle control-infected hUCB–MSCs (Supplementary Table 1). CCNA2 was reported to promote both G1/S and G2/M transitions [18]. Therefore, it is speculated that one of OCT4's functions in hUCB–MSCs is to regulate the cell cycle via transcriptional regulation of *CCNA2*.

The expression levels of many other genes were also altered by OCT4 inhibition of hUCB–MSCs. Among the genes identified, only four genes experienced statistically significant ($p < 0.05$) changes (Supplementary Figure 1B–E). Two genes that displayed increased gene expression in OCT4-inhibited hUCB–MSCs were *DTX1* and *FRAT1* (Supplementary Figure 1D, E). The up-regulation of DTX1, an inhibitor of NOTCH1 [19], may have contributed to the decreased adipogenic differentiation capacity of the OCT4-inhibited hUCB–MSCs, as inhibition of Notch1 expression or function can lead to the decreased expression of PPAR δ and γ, transcription factors that control adipogenic differentiation [20]. On a similar note, the expression levels of *HDAC2* and *4* were significantly decreased and *HDAC1* appeared to be down-regulated in OCT4-inhibited hUCB–MSCs as compared to controls (Fig. 4). Previous work has shown that the HDAC inhibitor tricostatin A inhibits adipogenesis, whereas the valproic acid analog valpromide, which does not possess HDAC inhibitory effects, does not prevent adipogenesis [21]. Therefore, HDAC regulation by OCT4 might be another mechanism by which adipogenic differentiation of hUCB–MSCs is indirectly controlled.

Specific knockdown of either *Oct4* or *Sox2* by RNA interference leads to a reduction in both genes' enhancer activities and endogenous expression levels, in addition to ESC differentiation [22]. A similar regulatory relationship may exist in hUCB–MSCs, as *SOX2* expression was noticeably decreased in OCT4-inhibited hUCB–MSCs. Other transcription factors, like *REX-1* and *c-MYC*, were also down-regulated but given that the expression of *ZNF 281* was not visibly altered. OCT4 probably only regulates a subset of the many transcription factors expressed in hUCB–MSCs. Oct4 also regulates Polycomb genes in mouse ESCs, including *Suz12* and *Bmi1* [23]. In mouse ESCs, *Suz12* and *Bmi1* expression levels were positively and negatively correlated with *Oct4* expression, respectively. Transcription of both *SUZ12* and *BMI1* was reduced in OCT4-inhibited hUCB–MSCs, suggesting that OCT4 has different chromatin modulating mechanisms in hUCB–MSCs and ESCs.

In this study, the expression of OCT4A in hUCB–MSCs was confirmed. We determined that OCT4 depletion significantly affects the biological activity of hUCB–MSCs in an *ex vivo* culture system. Inhibition of OCT4 expression in hUCB–MSCs resulted in the inhibition of cell proliferation and reduced multi-potency. As the field of adult stem cell therapy advances, different stem cell subtypes may offer insight into how MSC multipotency is maintained.

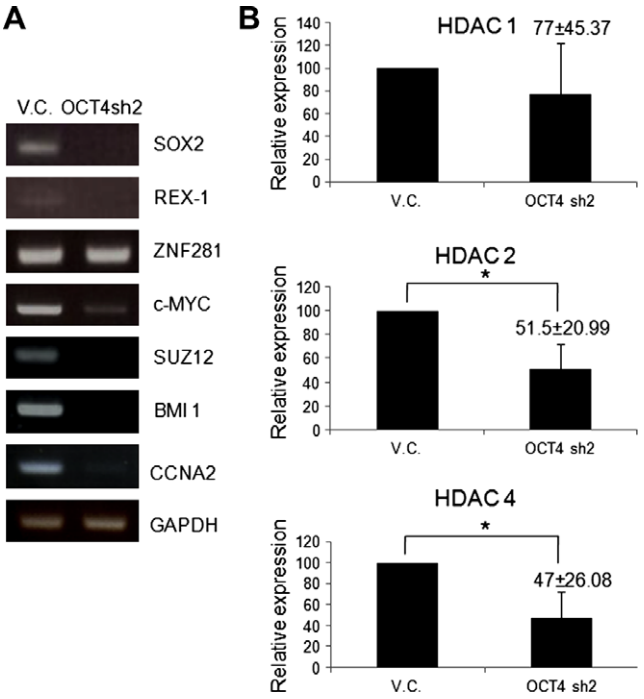


**Fig. 4.** Gene expression changes in OCT4-inhibited hUCB–MSCs. (A) RT-PCR analysis of OCT4-inhibited hUCB–MSCs and vehicle control-infected hUCB–MSCs. The expression levels of *SOX2*, *REX-1*, *c-MYC*, *SUZ12*, *BMI1* and *CCNA2* were obviously decreased in OCT4-inhibited hUCB–MSCs relative to the vehicle control-infected hUCB–MSCs. (B) Real-time RT-PCR of histone deacetylase genes (*HDAC*). The expression levels of *HDAC2* and *4* were significantly decreased in OCT4 inhibited hUCB–MSCs compared to the vehicle control-infected hUCB–MSCs. $^{*}p < 0.05$.

hUCB–MSCs in particular may prove to be a suitable cell type for the determination of the precise mechanism by which OCT4A contributes to the multi-potency of MSCs.

## Acknowledgment

Grant Support: Brain Korea 21 program, KOSEF grant funded by the Korean Government (MOST, No. M10641450002-06N4145-00200, M10641450002-6N4145-00210 and M10841000119-08 N4100-11910).

## Appendix A. Supplementary data

Supplementary data associated with this article can be found, in the online version, at doi:10.1016/j.bbrc.2009.04.094.

## References

[1] A. Erices, P. Conget, J.J. Minguell, Mesenchymal progenitor cells in human umbilical cord blood, Br. J. Haematol. 109 (2000) 235–242.
[2] S. Gronthos, D.M. Franklin, H.A. Leddy, P.G. Robey, R.W. Storms, J.M. Gimble, Surface protein characterization of human adipose tissue-derived stromal cells, J. Cell. Physiol. 189 (2001) 54–63.
[3] C. Campagnoli, I.A. Roberts, S. Kumar, P.R. Bennett, I. Bellantuono, N.M. Fisk, Identification of mesenchymal stem/progenitor cells in human first-trimester fetal blood, liver, and bone marrow, Blood 98 (2001) 2396–2402.
[4] M.S. Tsai, J.L. Lee, Y.J. Chang, S.M. Hwang, Isolation of human multipotent mesenchymal stem cells from second-trimester amniotic fluid using a novel two-stage culture protocol, Hum. Reprod. 19 (2004) 1450–1456.
[5] D.J. Prockop, Marrow stromal cells as stem cells for nonhematopoietic tissues, Science 276 (1997) 71–74.
[6] M. Pittenger, P. Vanguri, D. Simonetti, R. Young, Adult mesenchymal stem cells: potential for muscle and tendon regeneration and use in gene therapy, J. Musculoskelet. Neuronal Interact. 2 (2002) 309–320.
[7] S. Makino, K. Fukuda, S. Miyoshi, F. Konishi, H. Kodama, J. Pan, M. Sano, T. Takahashi, S. Hori, H. Abe, J. Hata, A. Umezawa, S. Ogawa, Cardiomyocytes can

be generated from marrow stromal cells in vitro, J. Clin. Invest. 103 (1999) 697–705.
[8] D.G. Phinney, I. Isakova, Plasticity and therapeutic potential of mesenchymal stem cells in the nervous system, Curr. Pharm. Des. 11 (2005) 1255–1265.
[9] P. Tropel, N. Platet, J.C. Platel, D. Noel, M. Albrieux, A.L. Benabid, F. Berger, Functional neuronal differentiation of bone marrow-derived mesenchymal stem cells, Stem Cells 24 (2006) 2868–2876.
[10] R. Bhatia, J.M. Hare, Mesenchymal stem cells: future source for reparative medicine, Congest. Heart Fail. 11 (2005) 87–91 (quiz 92–83).
[11] G.J. Pan, Z.Y. Chang, H.R. Scholer, D. Pei, Stem cell pluripotency and transcription factor Oct4, Cell Res. 12 (2002) 321–329.
[12] C.J. Lengner, F.D. Camargo, K. Hochedlinger, G.G. Welstead, S. Zaidi, S. Gokhale, H.R. Scholer, A. Tomilin, R. Jaenisch, Oct4 expression is not required for mouse somatic stem cell self-renewal, Cell Stem Cells 1 (2007) 403–415.
[13] V. Kotoula, S.I. Papamichos, A.F. Lambropoulos, Revisiting OCT4 expression in peripheral blood mononuclear cells, Stem Cells 26 (2008) 290–291.
[14] C.J. Lengner, G.G. Welstead, R. Jaenisch, The pluripotency regulator Oct4: a role in somatic stem cells?, Cell Cycle 7 (2008) 725–728
[15] T. Okamoto, T. Aoyama, T. Nakayama, T. Nakamata, T. Hosaka, K. Nishijo, T. Nakamura, T. Kiyono, J. Toguchida, Clonal heterogeneity in differentiation potential of immortalized human mesenchymal stem cells, Biochem. Biophys. Res. Commun. 295 (2002) 354–361.
[16] D. Baksh, R. Yao, R.S. Tuan, Comparison of proliferative and multilineage differentiation potential of human mesenchymal stem cells derived from umbilical cord and bone marrow, Stem Cells 25 (2007) 1384–1392.
[17] S. Liedtke, J. Enczmann, S. Waclawczyk, P. Wernet, G. Kogler, Oct4 and its pseudogenes confuse stem cell research, Cell Stem Cells 1 (2007) 364–366.
[18] M. Murphy, M.G. Stinnakre, C. Senamaud-Beaufort, N.J. Winston, C. Sweeney, M. Kubelka, M. Carrington, C. Brechot, J. Sobczak-Thepot, Delayed early embryonic lethality following disruption of the murine cyclin A2 gene, Nat. Genet. 15 (1997) 83–86.
[19] D.J. Izon, J.C. Aster, Y. He, A. Weng, F.G. Karnell, V. Patriub, L. Xu, S. Bakkour, C. Rodriguez, D. Allman, W.S. Pear, Deltex1 redirects lymphoid progenitors to the B cell lineage by antagonizing Notch1, Immunity 16 (2002) 231–243.
[20] C. Garces, M.J. Ruiz-Hidalgo, J. Font de Mora, C. Park, L. Miele, J. Goldstein, E. Bonvini, A. Porras, J. Laborda, Notch-1 controls the expression of fatty acid-activated transcription factors and is required for adipogenesis, J. Biol. Chem. 272 (1997) 29729–29734.
[21] D.C. Lagace, M.W. Nachtigal, Inhibition of histone deacetylase activity by valproic acid blocks adipogenesis, J. Biol. Chem. 279 (2004) 18851–18860.
[22] J.L. Chew, Y.H. Loh, W. Zhang, X. Chen, W.L. Tam, L.S. Yeap, P. Li, Y.S. Ang, B. Lim, P. Robson, H.H. Ng, Reciprocal transcriptional regulation of Pou5f1 and Sox2 via the Oct4/Sox2 complex in embryonic stem cells, Mol. Cell. Biol. 25 (2005) 6031–6046.
[23] P.A. Campbell, C. Perez-Iratxeta, M.A. Andrade-Navarro, M.A. Rudnicki, Oct4 targets regulatory nodes to modulate stem cell function, PLoS ONE 2 (2007) e553.